Design of a Schönflies motion generator using 4-RUU parallel manipulator

Ashwin BOSE and Jingjing LEI
Group-A

June 10, 2018

Contents

1 Introduction

Schönflies motion or displacement is a rigid body motion with three translations and one rotation about a fixed axis. Such 3T1R motion has many industrial applications as it is a common task to pick an object from a plane and place it at a different orientation in another parallel plane.

Parallel manipulators, with their high load carrying capacity, high rigidity, and low inertia are ideal for this application. Moreover, we use choose to design a lower mobility parallel manipulator as the situation demands a 4-dof motion. The aim of the project is to design a parallel system that outperforms the currently available Schönflies motion generators.

This paper is outlined as follows: First, in Section 2, the design problem is formulated as an optimization problem based on the given specifications. In Section 3, we explore different architectures of fully parallel manipulators performing 3T1R motion and a good candidate is chosen. Then in Section 4, the kinematic modelling of this candidate is performed. The dimensioning of the manipulator is performed in Section 4.3. Detail design and CAD modelling in CATIA is documented in Section 5

2 Task definition

The design specification for our model are given below:

- The robot must be capable of producing a test cycle that is commonly accepted for SCARA systems, in at most 500 ms. The test cycle consists of:
  - 25 mm vertical displacement upwards
  - 300 mm horizontal displacement with concomitant 90 degree turn
  - 25 mm vertical displacement downwards
  - 25 mm vertical displacement upwards
  - 300 mm horizontal displacement with a reverse 90 degree turn
  - 25 mm vertical displacement downwards
- The system should be capable of attaining a robust configuration
- The mechanism should not be too bulky

These customer requirements can be converted to the following functional requirements:

- The robot should have a $300 \times 100 \times 25$ mm workspace with the range of z-rotation of 90 degrees at every point

- The normalized forward and inverse Jacobians must be maximally invertible at every point in the workspace. In other words, their condition number should be as small as possible ($\kappa < 10$)
- The robot should have a the smallest link dimensions that can achieve the above requirements

The design problem can now be framed as an optimization problem as:

$$\begin{aligned} \text{minimize} \quad & \text{The sum of link lengths} \\ \text{subject to} \quad & 300 \times 300 \times 25 \text{ mm translation} \\ & 90 \text{ degree z-rotation} \\ & \text{Condition numbers } \kappa_1, \kappa_2 < 10 \end{aligned}$$

3 Conceptual design

Multiple architectures were considered for obtaining 3TR1 motion and the following 5 were shortlisted:

- 4-RUU [1]
- 2-RППR [2]
- 4-PRПRR [3]
- 3-PRRR,1ПРП [4]
- Quadrupetron [5]

3.1 Schönflies motion generators

4-RUU

The schematic of 4-RUU manipulator is shown in Fig. 1c. This manipulator has four links connecting the ground to the moving platform. Each limb consists of an active and a passive link. The ground and the active link are connected by a rotary joint with its axis parallel to the vertical axis. This link is connected by a universal joint to the passive link, which is in turn connected to the moving platform with another universal joint.

2-RППR

The schematic of this robot is shown in Fig. 1a. The moving plate carrying the operation point P is coupled to the base frame by means of two identical limbs. Each limb is a serial

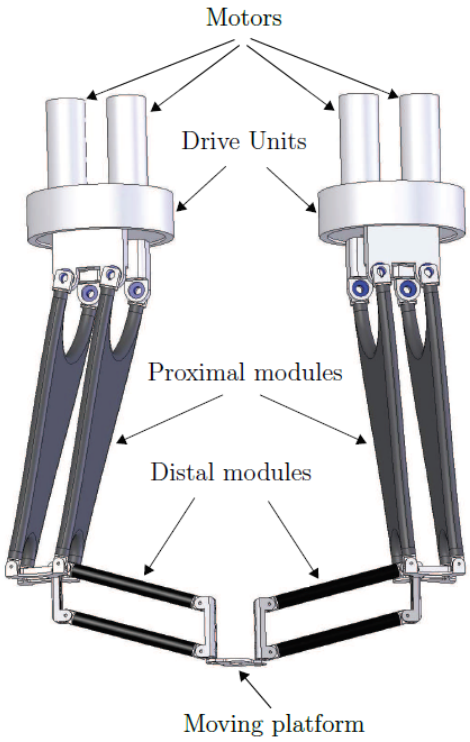

(a) Schematic of 2-RΠΠΠR parallel manipulator

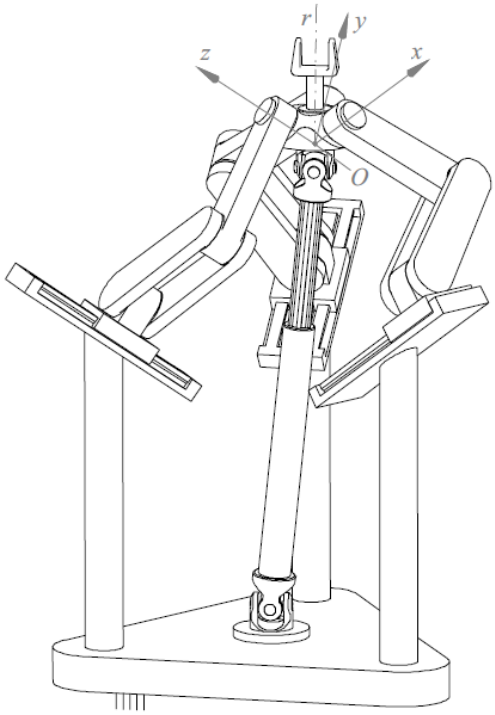

(b) Schematic of 3-PRRR,1ΠPΠ parallel manipulator

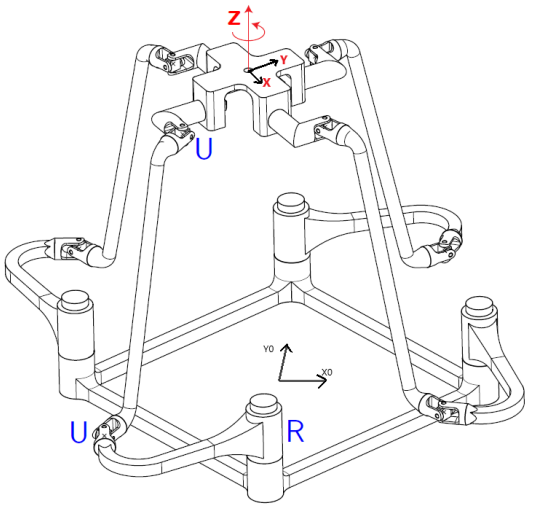

(c) Schematic of 4-RUU parallel manipulator

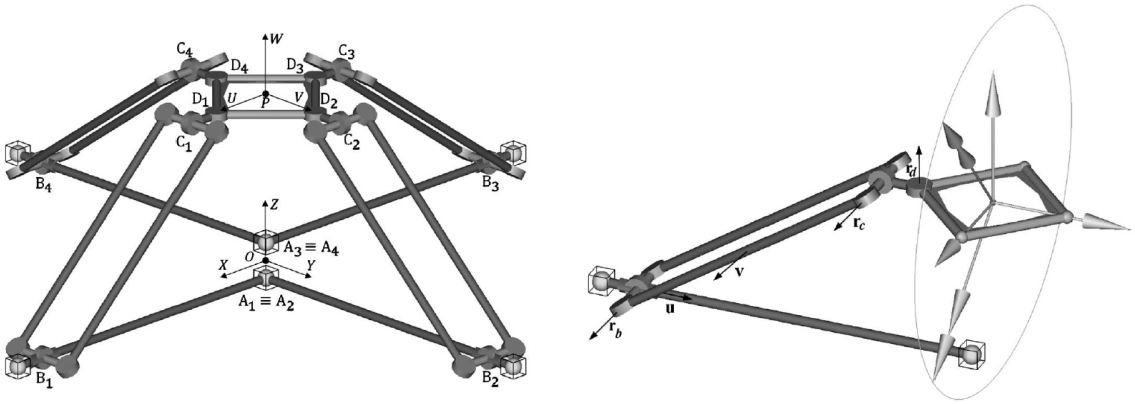

(a) Schematic representation (b) Kinematic modelling of a leg

Figure 2: PRΠRR manipulator

chain of RΠΠR type, with Π indicating a parallelogram linkage.

In each limb, the first link is connected to the ground using an actuated rotary joint oriented along the vertical axis. This link is connected to the second link through another actuated joint oriented along the horizontal plane. Both the actuators can be grounded by designing a good transmission mechanism, thereby giving it the properties of a fully parallel manipulator.

4-PRΠRR

The schematic is shown in Fig. 2a. This manipulator has 4 identical legs that connects the moving platform to the base. The base is connected to the actuated prismatic joint. This joint is connected to a Π type passive link through a rotary joint, which is oriented along an axis (r_b) perpendicular to the active joint axis as shown in Fig. 2b. The Π leg is connected to another joint at r_c to a second passive leg. This passive leg is connected to the platform with a rotary joint at r_d.

3-PRRR,1ΠPΠ

This manipulator is different from the others in the sense that the translation of the platform is decoupled from its rotation. The three PRRR legs lead to pure translation whereas the ΠPΠ leg (a telescopic double universal joint chain) does the rotation. The translations is obtained by a PRRR link, where the base is connected to the first link by an actuated prismatic joint. This link is connected to the platform through 2 passive joints as shown in Fig. 1b.

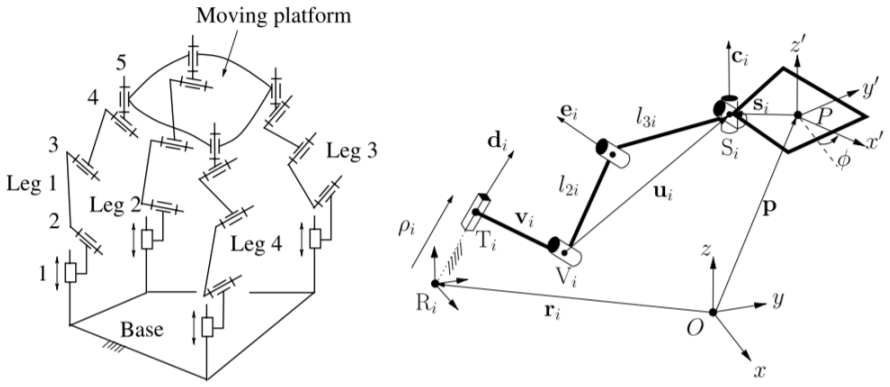

(a) Schematic representation.

(b) Kinematic modeling of a leg.

Figure 3: Quadrupetron

	4-RUU	2-RΠΠR	4-PRΠRR	3-PRRR,1ΠPΠ	Quadrupetron
K_N	0.76	0.76	0.9	0.70	0.82
K_L	0.9	0.68	0.9	0.9	0.9
K_J	0.52	0.52	0.58	0.63	0.60
K_B	0.43	0.31	0.56	0.38	0.65
K	0.65	0.57	0.73	0.65	0.74

Table 1: Complexity analysis

Quadrupetron

Quadrupetron is a 4-PRUU manipulator with actuated prismatic joints. As shown in Fig. 3, the moving platform is connected to the base via a PRUU leg. The prismatic joints are oriented along different edges of cuboidal frame.

3.2 Complexity analysis

The complexity analysis [6] of the chosen architectures is performed in this section. The results are tabulated in Table. 1.

An architecture was now chosen from the list based on the following criterion:

- Rotary actuators are preffered over prismatic actuators
- No floating prismatic should be used
- Simple kinematic structure

Finally, 4-RUU was chosen.

4 Embodiment

4.1 Position kinematics

The 4-RUU manipulator has four identical legs. The schematic of a leg is shown in Fig. 4a. The inverse kinematic problem is the problem of finding the configuration of the manipulator given the pose of the end-effector.

In 4-RUU robot, the configuration space is defined as:

$$\mathbf{X} = (x, y, z, \theta_z) \tag{1}$$

The geometry of the manipulator is such that it doesn't rotate about x-y plane. The location of the actuators:

$$\begin{aligned} \mathbf{A}_1 &= \begin{bmatrix} b & 0 & 0 \end{bmatrix}^\top \\ \mathbf{A}_2 &= \begin{bmatrix} 0 & b & 0 \end{bmatrix}^\top \\ \mathbf{A}_3 &= \begin{bmatrix} -b & 0 & 0 \end{bmatrix}^\top \\ \mathbf{A}_4 &= \begin{bmatrix} 0 & -b & 0 \end{bmatrix}^\top, \end{aligned} \tag{2}$$

where b is the circumradius of the square that connects the base points. The coordinates of the end-effector corners in local coordinates system e:

$$\begin{aligned} {}^e\mathbf{C}_1 &= \begin{bmatrix} a & 0 & 0 \end{bmatrix}^\top \\ {}^e\mathbf{C}_2 &= \begin{bmatrix} 0 & a & 0 \end{bmatrix}^\top \\ {}^e\mathbf{C}_3 &= \begin{bmatrix} -a & 0 & 0 \end{bmatrix}^\top \\ {}^e\mathbf{C}_4 &= \begin{bmatrix} 0 & -a & 0 \end{bmatrix}^\top, \end{aligned} \tag{3}$$

The position of the corners of the end effector in global coordinate system, C_i can be calculated as:

$$\mathbf{C}_i = \mathbf{X}_{pos} + \mathbf{R}_z(\theta_z)\ {}^e\mathbf{C}_i \tag{4}$$

where,

$$\mathbf{R}_z(\theta_z) = \begin{bmatrix} \cos(\theta) & -\sin(\theta) & 0 \\ \sin(\theta) & \cos(\theta) & 0 \\ 0 & 0 & 1 \end{bmatrix}$$

and, $\mathbf{X}_{pos}$ is the Cartesian coordinates of the centre of the platform $[x, y, z]^\top$.

$\mathbf{A}_i$ and $\mathbf{C}_i$ are connected by an active link AB and passive link BC as shown in Fig. 4a of known lengths, l and r respectively. Finding $\mathbf{B}_i$ can be reduced to a circle-sphere intersection problem. A schematic of this problem is shown in Fig. 4b.

Now we have got the position of all the necessary joints, we can move ahead to solve the velocity kinematics problem.

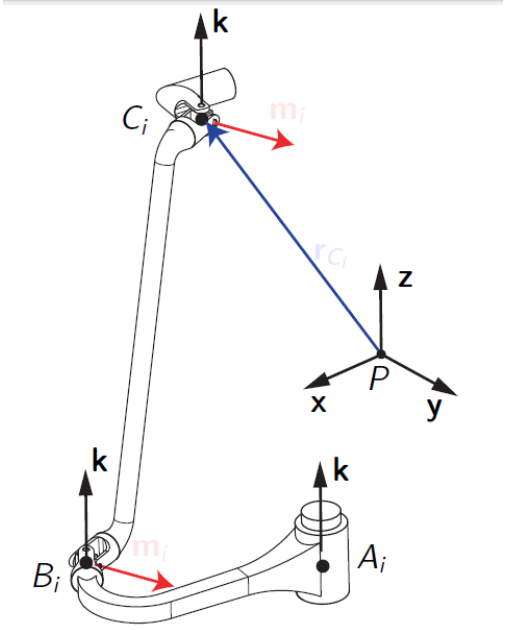

(a) Schematic of legs of 4-RUU parallel manipulator

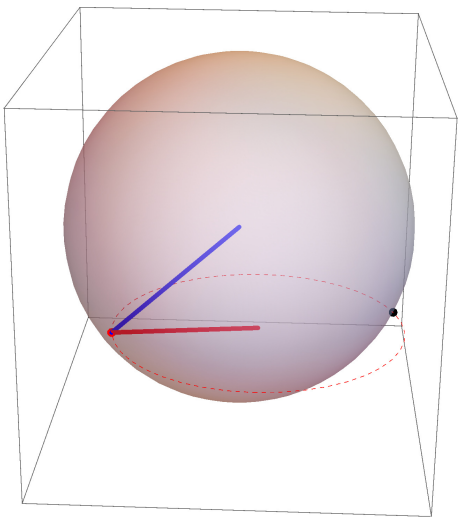

(b) Circle-sphere intersection problem. Solutions are represented by a blue dot and a red dot. **A** and **C** are connected through the red dot by the active (red) link and passive (blue) link

4.2 Velocity kinematics

In this section, we use screw theory to solve the first order inverse kinematics of 4-RUU manipulator. First, we define the limb twist system of every leg of the manipulator (see Fig. 4a).

The following twists form the basis of the limb twist system:

$$\hat{\epsilon}_{0i1} = \begin{bmatrix} \mathbf{k} \\ \mathbf{r}_{Ai} \times \mathbf{k} \end{bmatrix}, \hat{\epsilon}_{0i2} = \begin{bmatrix} \mathbf{k} \\ \mathbf{r}_{Bi} \times \mathbf{k} \end{bmatrix}, \hat{\epsilon}_{0i3} = \begin{bmatrix} \mathbf{m}_i \\ \mathbf{r}_{Bi} \times \mathbf{m}_i \end{bmatrix},$$
$$\hat{\epsilon}_{0i4} = \begin{bmatrix} \mathbf{m}_i \\ \mathbf{r}_{Ci} \times \mathbf{m}_i \end{bmatrix}, \hat{\epsilon}_{0i5} = \begin{bmatrix} \mathbf{k} \\ \mathbf{r}_{Ci} \times \mathbf{k} \end{bmatrix} \tag{5}$$

The limb constraint wrench system is:

$$\hat{\tau}^c_{\infty i} = \begin{bmatrix} \mathbf{0}_3 \\ \mathbf{k} \times \mathbf{m}_i \end{bmatrix} \tag{6}$$

Combining the limb constraint wrenches of all the limbs, we get the following 2-system of wrenches of the platform:

$$\begin{aligned} \mathbf{W}_c &= \text{span}(\hat{\tau}^c_{\infty 1}, \hat{\tau}^c_{\infty 2}, \hat{\tau}^c_{\infty 3}, \hat{\tau}^c_{\infty 4}) \\ &= \text{span}(\hat{\tau}^c_{\infty x}, \hat{\tau}^c_{\infty y}) \end{aligned} \tag{7}$$

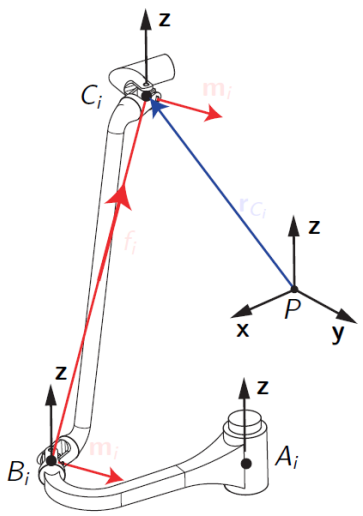

Figure 5: Actuation wrench: 4RUU

We find the twist of the platform as the reciprocal of the constraint wrenches.

$$\mathbf{T} = \text{span}(\hat{\epsilon_{\infty x}}, \hat{\epsilon_{\infty y}}, \hat{\epsilon_{\infty z}}, \hat{\epsilon_{0z}}) \tag{8}$$

As predicted, the motion is of the type 3T1R.

We now calculate the actuation wrench system of this manipulator. For this, we need to find a screw that is reciprocal to all the twists except for the actuation twist. A as shown in Fig. 5 screw directed along the two passive joints. Actuation wrench system of the leg i was found as :

$$\hat{\tau_{0a}^i} = \begin{bmatrix} \mathbf{f}_i \\ \mathbf{r}_{Ci} \times \mathbf{f}_i \end{bmatrix} \tag{9}$$

The actuation wrench system of the manipulator,

$$W = \text{span}(\hat{\tau}_{0a}^1, \hat{\tau}_{0a}^2, \hat{\tau}_{0a}^3, \hat{\tau}_{0a}^4) \tag{10}$$

This is a 4-system. From this we see that the global wrench system is a 6-system.

Moving platform twist:

$$\mathbf{t} = \begin{bmatrix} \omega \\ \dot{\mathbf{p}} \end{bmatrix} = \Sigma \hat{\epsilon}_{0ij} \dot{\theta}; \qquad i = 1..4 \tag{11}$$

Pre-multiplying these equations with the corresponding actuation wrenches gives:

$$\hat{\tau}_{0a}^i \circ \mathbf{t} = \hat{\tau}_{0a}^i \circ \hat{\epsilon}_{0i1} \dot{\theta}_{i1}; \quad i = 1..4 \tag{12}$$

$$[(\mathbf{r}_{Ci} \times \mathbf{f}_i^\top)\mathbf{f}_i^\top]\mathbf{t} = (A_i C_i \times \mathbf{f}_i)\mathbf{k}\dot{\theta}_{i1} \tag{13}$$

The reciprocal products between constraint wrenches and moving platform twist gives us:

$$\hat{\tau}^{c}_{\infty i} \circ \mathbf{t} = 0 \tag{14}$$

$$\mathbf{k} \times \mathbf{m}_i = 0 \tag{15}$$

Equations 13 and 15 can be written in matrix form as:

$$\mathbf{A}\mathbf{t} = \mathbf{B}\dot{\theta} \tag{16}$$

with $\dot{\theta} = [\theta_{11}, \theta_{21}, \theta_{31}, \theta_{41}]^\top$. Where,

$$\mathbf{A} = \begin{bmatrix} (\mathbf{r}_{C1} \times \mathbf{f}_1^\top) & \mathbf{f}_1^\top \\ (\mathbf{r}_{C2} \times \mathbf{f}_2^\top) & \mathbf{f}_2^\top \\ (\mathbf{r}_{C3} \times \mathbf{f}_3^\top) & \mathbf{f}_3^\top \\ (\mathbf{r}_{C4} \times \mathbf{f}_4^\top) & \mathbf{f}_4^\top \\ \mathbf{k} \times \mathbf{m}_1 & \mathbf{0}_3^\top \\ \mathbf{k} \times \mathbf{m}_2 & \mathbf{0}_3^\top \\ \mathbf{k} \times \mathbf{m}_3 & \mathbf{0}_3^\top \\ \mathbf{k} \times \mathbf{m}_4 & \mathbf{0}_3^\top \end{bmatrix}, \mathbf{B} = \begin{bmatrix} (A_1C_1 \times \mathbf{f}_1)\mathbf{k} & 0 & 0 & 0 \\ 0 & (A_2C_2 \times \mathbf{f}_2)\mathbf{k} & 0 & 0 \\ 0 & 0 & (A_3C_3 \times \mathbf{f}_3)\mathbf{k} & 0 \\ 0 & 0 & 0 & (A_4C_4 \times \mathbf{f}_4)\mathbf{k} \\ 0 & 0 & 0 & 0 \\ 0 & 0 & 0 & 0 \\ 0 & 0 & 0 & 0 \\ 0 & 0 & 0 & 0 \end{bmatrix} \tag{17}$$

A and **B** are defined as the forward Jacobian and the inverse Jacobian respectively. The singularities of these matrices correspond to the gain and loss singularities of the robot. These matrices characterize the performances of the manipulator at a configuration. This can be represented using condition numbers.

One should note that the different columns of these matrices have different dimensions. We should normalize these matrices to obtain a meaningful information from the condition number. We use the radius of the base circle, l as the characteristic length of normalization.

The new normalized Jacobian matrices are obtained by dividing all the columns with unit of length by the characteristic length, and are denoted by $\mathbf{A}_n$ and $\mathbf{B}_n$

4.3 Dimensioning

In this section, we perform the dimensioning of the robot by solving the optimization problem defined in Section. 2.

The design variables of the problem are:

- b, radius of the base circle,
- l, length of the active link,
- r, length of the passive link,

Table 2: Optimization results

b (mm)	l (mm)	r (mm)	a(mm)	x_{mid}(mm)	y_{mid}(mm)	z_{mid}(mm)	θ_{mid} (rad)
928	662	836	322	-146	22	292	0.012

- a, radius of the top platform,
- x_0, x co-ordinate of the home position,
- y_0, y co-ordinate of the home position,
- z_0, z co-ordinate of the home position,
- θ_0, θ_z value of the home position.

The robot should be as compact as possible, therefore the objective function was defined as:

$$F(X) = b + l + r + a \tag{18}$$

The robot must have a workspace of $300 \times 100 \times 25$ with 90 degree rotation at every point. The workspace was discretized and the normalized Jacobians were calculated at all these discrete points, and their max values were stored. The discretizations chosen were, 10 mm for lengths and 10 degrees for angles. The constraints were defined as:

$$C_1 = 10 - \max(\kappa(\mathbf{A}))$$
$$C_2 = 10 - \max(\kappa(\mathbf{B})) \tag{19}$$
$$C_3 = l - \frac{b}{\sqrt{2}} \tag{20}$$

C_1 and C_2 ensure that the manipulator has a good performance everywhere within the workspace. C_3 prevents link intersection.

Optimization was performed using genetic algorithm. The results obtained are tabulated in Table. 2.

5 Detail design

The detail design of the robot is discussed in this section. The following is the hierarchy of design:

- 4RUU assembly
  - Base platform
  - Moving platform

- Limb sub-assembly (4 units)
  - Active joint
  - Passive joint
  - U-joint

Images of these components are shown in Fig. 6.

6 Conclusion

Schönflies motion generators has a wide range of applications in the industry. In this project, we designed as well as detailed the design methodology of a Schönflies motion generator. A series of architectures that could generate Schönflies motion were studied and the complexity analysis was performed for a selected few. 4-RUU parallel manipulator was selected after this comparison.

In the embodiment stage of design, we optimized the dimensions of the manipulator to attain the design requirements. The kinematic analysis of the manipulator was performed to find its forward and inverse Jacobians. We found the link dimensions for the manipulators with a desired workspace (condition number less than 10).

A detail design of the robot and an animation of it performing a pick and place motion was made in SOLIDWORKS. We thereby successfully designed a product satisfying all the requirements of the customer.

(a) Assembly

(b) Base platform

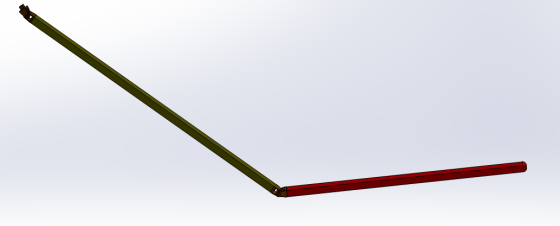

(c) Link assembly

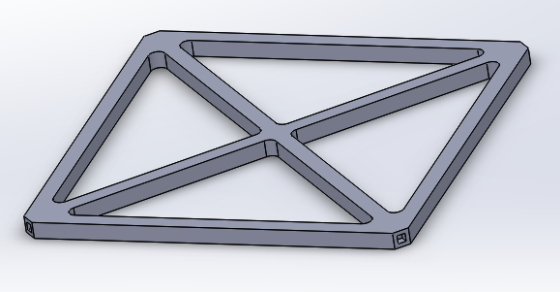

(d) Moving platform

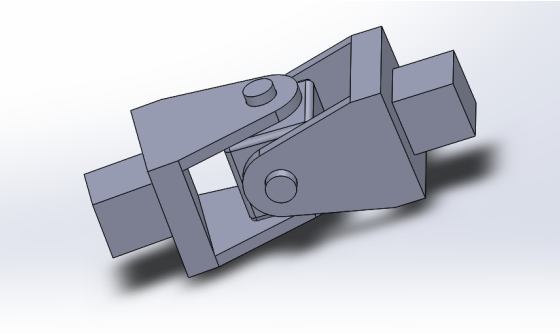

(e) U-joint

Figure 6: CAD-4RRU robot

Bibliography

[1] Semaan Amine, Mehdi Tale Masouleh, Stéphane Caro, Philippe Wenger, and Clément M Gosselin. Singularity analysis of the 4-ruu parallel manipulator using grassmann-cayley algebra. *Transactions of the canadian society for mechanical engineering*, 35(5):515–528, 2011.

[2] Jorge Angeles, Stéphane Caro, Waseem Khan, and Alexis Morozov. The design and prototyping of an innovative schönflies motion generator. *Proceedings of the Institution of Mechanical Engineers. Part C, Journal of Mechanical Engineering Science*, 220(C7):935–944, 2006.

[3] Oscar Salgado, Oscar Altuzarra, Víctor Petuya, and Alfonso Hernández. Synthesis and design of a novel 3t1r fully-parallel manipulator. *Journal of Mechanical Design*, 130(4):042305, 2008.

[4] Grigore Gogu. Fully-isotropic t3r1-type parallel manipulators. *On Advances in Robot Kinematics*, pages 265–272, 2004.

[5] Xianwen Kong and Clément Gosselin. Forward displacement analysis of a quadratic 4-dof 3t1r parallel manipulator. *Meccanica*, 46(1):147–154, Feb 2011.

[6] Jorge Angeles, Waseem A Khan, Stéphane Caro, and Damiano Pasini. The concpetual design of robotic architectures by means of a complexity measure. *McGill University, Institut de Recherche en Communications et Cybernetique de Nantes*, 2010.